

## Scaling Regimes and the Singularity of Specific Heat in the 3D Ising Model

J. Kaupužs<sup>1,2,\*</sup>, R. V. N. Melnik<sup>3</sup> and J. Rimšāns<sup>1,2</sup>

<sup>1</sup> Institute of Mathematics and Computer Science, University of Latvia,  
29 Raiņa Boulevard, LV1459, Riga, Latvia.

<sup>2</sup> Institute of Mathematical Sciences and Information Technologies,  
University of Liepaja, 14 Liela Street, Liepaja LV-3401, Latvia.

<sup>3</sup> Wilfrid Laurier University, Waterloo, Ontario, Canada, N2L 3C5.

Received 24 May 2012; Accepted (in revised version) 12 September 2012

Communicated by Michel A. Van Hove

Available online 12 December 2012

---

**Abstract.** The singularity of specific heat  $C_V$  of the three-dimensional Ising model is studied based on Monte Carlo data for lattice sizes  $L \leq 1536$ . Fits of two data sets, one corresponding to certain value of the Binder cumulant and the other — to the maximum of  $C_V$ , provide consistent values of  $C_0$  in the ansatz  $C_V(L) = C_0 + AL^{\alpha/\nu}$  at large  $L$ , if  $\alpha/\nu = 0.196(6)$ . However, a direct estimation from our  $C_V^{\max}$  data suggests that  $\alpha/\nu$ , most probably, has a smaller value (e.g.,  $\alpha/\nu = 0.113(30)$ ). Thus, the conventional power-law scaling ansatz can be questioned because of this inconsistency. We have found that the data are well described by certain logarithmic ansatz.

**AMS subject classifications:** 65C05, 82B20, 82B80, 82B27

**Key words:** Ising model, Monte Carlo simulation, specific heat, finite-size scaling, critical exponents.

---

## 1 Introduction

The standard three-dimensional (3D) Ising model, as well as several models of the 3D Ising universality class, have been extensively studied by the Monte Carlo (MC) method in past (see, e.g., [1, 2] and references therein) with an aim to evaluate the critical exponents. Some cornerstone works are due to J. Chen et al. [3] and H. W. J. Blöte et al. [4]. More recent works are [5–7, 28]. In [5], the singularity of specific heat of the classical 3D

---

\*Corresponding author. Email addresses: kaupuzs@latnet.lv (J. Kaupužs), rmelnik@wlu.ca (R. V. N. Melnik), rimshans@mii.lu.lv (J. Rimšāns)

Ising model is studied, which is also the main subject of our current MC study. In [6,7], modified models with the so-called improved Hamiltonian are considered. The basic idea of this method is to choose such Hamiltonian, for which the leading corrections to scaling vanish. It is believed that good estimates of the critical exponents can be therefore extracted from these models by simulating even relatively small lattices. The improved Hamiltonian has to be a good approximation of the fixed-point-Hamiltonian of an exact renormalization group (RG) transformation to ensure that this method works well. Since we do not strictly know whether this condition is really satisfied, here we prefer to use a simple strategy — to simulate very large lattices. It is reasonable to choose the simplest model of the actual universality class, i.e., the classical 3D Ising model, to obtain good results (good simulation data for maximally large lattice size  $L$ ) by this approach. A model including next-nearest-neighbor interactions has been considered in [4] as a good alternative to the classical Ising model, using a coupling to next-nearest neighbors as a parameter to minimize corrections to scaling. However, in some cases corrections to scaling seem to be negligible also in the classical Ising model with nearest-neighbor coupling. An example is the scaling consistency test, considered in Section 3. From this point of view, our choice of the classical 3D Ising model also could be quite good.

Usually, lattices of linear sizes  $L$  up to  $L = 128$  are simulated [1]. However, much larger lattices can be well simulated on modern computers, and MC results for susceptibility and magnetization cumulant at  $L \leq 1536$  have been recently reported in [8]. Some simulation results for even larger lattices have been reported in literature (see, e.g., [9] for a review). A distinguishing feature of our simulations of very large lattices is a high enough (moderately high) statistics, which is sufficient for a finite-size scaling analysis in the critical region with an aim to estimate the critical exponents. It has been found in [8] that the data can be well fit with critical exponents  $\eta = \omega = 1/8$  and  $\nu = 2/3$ , which are consistent with the GFD (grouping of Feynman diagrams) theory of [10,11], confirmed and appreciated also in [12], and are remarkably different from those of the perturbative RG theory, i.e.,  $\eta = 0.0335 \pm 0.0025$ ,  $\omega = 0.799 \pm 0.011$  and  $\nu = 0.6304 \pm 0.0013$  [13]. These results, however, are not strictly conclusive, since the fits with both sets of the exponents are quite acceptable. A minor problem for the perturbative RG scaling is that some fits of the susceptibility data of [8], assuming  $\omega \approx 0.8$ , give slightly larger values of  $\eta$  (e.g., 0.0397(28) and 0.0405(25)) than  $\eta = 0.0335 \pm 0.0025$ . Here we go substantially beyond the results of [8] by completing a comprehensive study on specific heat data to obtain more conclusive evidences for a better distinguishing between the two possible scaling scenario.

## 2 Simulation results

We have simulated the 3D Ising model on simple cubic lattice with

$$H/T = -\beta \sum_{\langle ij \rangle} \sigma_i \sigma_j, \quad (2.1)$$

where  $H$  is the Hamiltonian,  $T$  is the temperature measured in energy units,  $\beta$  is the coupling constant and  $\langle ij \rangle$  denotes the pairs of neighboring spins  $\sigma_i = \pm 1$  in the 3D lattice with periodic boundary conditions. The MC simulations have been performed with the Wolff single cluster algorithm [14], using its parallel implementation described in [15].

The quantities of current interest are specific heat  $C_V$  and its derivatives, i.e.,

$$C_V = N (\langle \varepsilon^2 \rangle - \langle \varepsilon \rangle^2), \quad (2.2)$$

$$C'_V = N^2 (3\langle \varepsilon \rangle \langle \varepsilon^2 \rangle - \langle \varepsilon^3 \rangle - 2\langle \varepsilon \rangle^3), \quad (2.3)$$

$$C''_V = N^3 (12\langle \varepsilon \rangle^2 \langle \varepsilon^2 \rangle - 3\langle \varepsilon^2 \rangle^2 - 4\langle \varepsilon \rangle \langle \varepsilon^3 \rangle - 6\langle \varepsilon \rangle^4 + \langle \varepsilon^4 \rangle), \quad (2.4)$$

calculated from the Boltzmann statistics, where  $N = L^3$  is the total number of spins and  $\varepsilon$  is the energy per spin.

In [8], our MC simulation results at certain pseudo-critical coupling  $\tilde{\beta}_c(L)$ , corresponding to  $U = \langle m^4 \rangle / \langle m^2 \rangle^2 = 1.6$  have been reported for lattice sizes  $16 \leq L \leq 1536$ . Here  $m$  is the magnetization per spin, and  $1 - U/3$  is the Binder cumulant. As already explained in [15],  $\tilde{\beta}_c(L)$  tends to the true critical coupling  $\beta_c$  at  $L \rightarrow \infty$  for any fixed  $1 < U < 3$ . Therefore, the precise value of  $U$  is not important in our following scaling analysis. At  $\beta = \beta_c$ , the ratio  $U$  tends to certain universal value  $U^* \approx 1.6$  [1,20] when  $L \rightarrow \infty$ . The value  $U = 1.6$  has been chosen to obtain pseudo-critical couplings closer to  $\beta_c$ . We have evaluated  $C_V$  at  $\beta = \tilde{\beta}_c(L)$  from these simulations by the same techniques as described in [8]. The results are listed in Table 1.

Table 1: The values of specific heat  $C_V$  depending on  $L$  at  $\beta = \tilde{\beta}_c(L)$ , where  $\tilde{\beta}_c(L)$  corresponds to  $U = 1.6$ .

L	$\tilde{\beta}_c(L)$	$C_V$	L	$\tilde{\beta}_c(L)$	$C_V$
1536	0.2216546081(114)	118.40(75)	128	0.22165430(20)	66.27(15)
1280	0.2216546524(136)	114.40(82)	108	0.22165376(26)	63.22(14)
1024	0.221654625(22)	107.79(84)	96	0.22165369(32)	61.47(13)
864	0.221654635(25)	104.45(59)	80	0.22165278(32)	58.421(95)
768	0.221654672(27)	101.47(54)	64	0.22165159(52)	55.162(83)
640	0.221654615(31)	97.38(43)	54	0.22164968(56)	52.582(84)
512	0.221654662(45)	92.31(37)	48	0.22164790(69)	50.872(67)
432	0.221654637(58)	89.27(36)	40	0.22164383(80)	48.275(57)
384	0.221654567(65)	86.56(35)	32	0.22163444(98)	45.086(50)
320	0.221654716(75)	83.13(30)	27	0.2216212(11)	42.718(42)
256	0.22165460(11)	78.57(30)	24	0.2216125(12)	41.265(35)
216	0.22165460(13)	75.51(20)	20	0.2215821(17)	38.772(29)
192	0.22165425(16)	73.02(24)	16	0.2215235(18)	35.914(20)
160	0.22165414(18)	69.94(19)			

We have performed new MC simulations for  $8 \leq L \leq 1024$  to evaluate maximal values of specific heat  $C_V^{\max}$ . The maximum of  $C_V$  is located at certain pseudo-critical coupling  $\hat{\beta}_c = \hat{\beta}_c(L)$ . For each  $L$ , we have found a good initial approximation  $\beta_0$  for  $\hat{\beta}_c(L)$ , and then

have evaluated  $\hat{\beta}_c(L)$  and  $C_V^{\max}$  from the simulations at  $\beta = \beta_0$  by using truncated Taylor expansion

$$C_V(\beta) \simeq C_V(\beta_0) + C'_V(\beta_0)(\beta - \beta_0) + \frac{1}{2}C''_V(\beta_0)(\beta - \beta_0)^2. \quad (2.5)$$

The truncation errors are negligible as compared to the statistical errors, since the  $C_V^{\max} - C_V(\beta_0)$  values are sufficiently small. Namely, only in the worst case of  $L = 768$  this difference is about  $1.46\sigma$ , where  $\sigma$  is the standard error, whereas in other cases it is remarkably smaller than  $\sigma$ . Comparing the values of  $C_V(\tilde{\beta}_c)$  in Table 1 with those calculated from (2.5), we have verified that  $C_V(\beta_0) - C_V(\tilde{\beta}_c)$  can be estimated with about 5 percent accuracy from this expansion around  $\beta = \beta_0$ . Since  $|\beta_0 - \hat{\beta}_c| \ll |\beta_0 - \tilde{\beta}_c|$ , the relative truncation errors for  $C_V^{\max} - C_V(\beta_0)$  are even much smaller, i.e., the truncation errors for  $C_V^{\max}$  are, indeed, much smaller than  $\sigma$ .

The initial approximations of  $\hat{\beta}_c$ , i.e.,  $\beta_0$  (see Table 2) have been estimated for a subset of sizes  $L \leq 128$  by using an iteration scheme, which is analogous to the one used in [8] for finding  $\tilde{\beta}_c$ . Unfortunately, it is difficult to ensure small enough fluctuations in such an iteration scheme for  $\hat{\beta}_c$  at larger system sizes. Therefore, an appropriate value of  $\beta_0$  for any  $L > 128$  has been obtained by a finite-size extrapolation from  $\hat{\beta}_c(L')$  data with  $L' < L$ .

Table 2: The maximal values of specific heat  $C_V^{\max}$  and the corresponding pseudo-critical couplings  $\hat{\beta}_c$ , evaluated from the simulations at  $\beta = \beta_0$ , depending on the linear system size  $L$ .

L	$\beta_0$	$\hat{\beta}_c$	$C_V^{\max}$
1024	0.2216585	0.22165903(16)	134.96(72)
768	0.2216607	0.22166213(23)	127.57(69)
640	0.2216635	0.22166359(31)	121.37(66)
512	0.2216673	0.22166679(40)	117.28(62)
384	0.2216747	0.22167526(52)	109.24(51)
320	0.2216819	0.22168192(69)	104.94(48)
256	0.2216929	0.22169312(76)	100.38(37)
192	0.2217151	0.2217149(10)	92.90(28)
160	0.22173663	0.2217347(14)	89.12(25)
128	0.2217708	0.2217742(16)	84.25(22)
96	0.2218383	0.2218366(24)	78.81(20)
80	0.2218992	0.2219002(32)	75.11(19)
64	0.2220053	0.2220057(42)	71.36(17)
48	0.2222013	0.2221987(58)	66.07(15)
40	0.2223714	0.2223761(76)	62.57(14)
32	0.2226726	0.222659(10)	58.66(14)
24	0.2232	0.223195(12)	53.76(10)
20	0.223666	0.223686(13)	50.505(82)
16	0.224436	0.224443(15)	46.596(65)
12	0.225771	0.225813(16)	41.420(47)
10	0.227051	0.226903(18)	38.187(39)
8	0.228561	0.228567(20)	34.108(31)

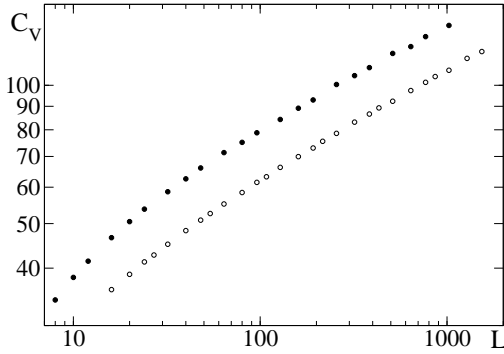


Figure 1: Specific heat  $C_V$  of the 3D Ising model depending on the lattice size  $L$ . Empty circles correspond to the  $C_V$  data at  $\beta = \hat{\beta}_c(L)$ , i.e.  $U = 1.6$ , whereas solid circles — to the  $C_V^{\max}$  data. Statistical errors are within the symbol size.

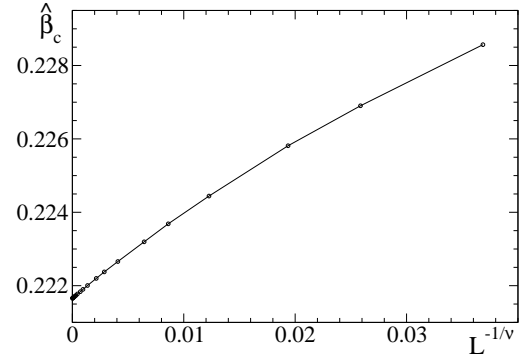


Figure 2: The pseudocritical coupling  $\hat{\beta}_c$  as a function of  $L^{-1/\nu}$  at  $\nu = 0.63$ . Statistical errors are within the symbol size.

Calculations of the second derivative  $C_V''(\beta_0)$  from (2.4) yield sufficiently accurate values for  $L \leq 384$  (e.g.,  $-0.920(23) \times 10^8$ ,  $-0.926(30) \times 10^9$ ,  $-0.923(38) \times 10^{10}$  and  $-1.054(76) \times 10^{11}$  at  $L = 48, 96, 192$  and  $384$ , respectively), but the errors remarkably increase for larger sizes because of the statistical simulation errors and also numerical rounding errors. Indeed, the expression (2.4) contains the proportionality coefficient  $N^3$ , which exceeds  $C_V''$  by many orders of magnitude at the largest sizes, i.e., about  $5 \times 10^{14}$  times at  $L = 1024$ . It means that separate terms in (2.4) almost cancel each other. This is a typical situation, where the relative errors can become large because of the numerical rounding. The values of  $C_V''$  for  $L > 384$  have been quite accurately estimated from  $\ln C_V''$  vs  $\ln L$  fit. The small errors ( $\sim 4\%$ ) in these values practically do not affect the results for  $C_V^{\max}$ , listed in Table 2. Indeed,  $C_V''$  enters only the very small correction term in (2.5), which does not exceed in magnitude the value about 1.46 standard deviations of  $C_V$ .

As in [8], the simulations at several sizes  $L$  have been performed with two different pseudo-random number generators (the same ones as in [8]), and a good consistency has been found, further increasing the confidence about our results.

The  $C_V$  plots in the log-log scale are shown in Fig. 1. In Fig. 2, the pseudocritical coupling  $\hat{\beta}_c$  is plotted as a function of  $L^{-1/\nu}$ , using the known estimate  $\nu \approx 0.63$  for the correlation length critical exponent  $\nu$ . Such a plot has to be linear at  $L^{-1/\nu} \rightarrow 0$ , if the value of  $\nu$  is chosen correctly.

### 3 A scaling consistency test

According to the predictions of the perturbative RG theory (see, e.g., [13, 16–20]) and finite-size scaling theory, specific heat of the 3D Ising model obeys a power-law asymptotic ansatz

$$C_V = C_0 + |t|^{-\alpha} f(tL^{1/\nu}) \quad \text{at } t \rightarrow 0 \quad (3.1)$$

for any given  $tL^{1/\nu}$ , where  $t = (\beta_c - \beta)/\beta_c$  is the reduced temperature,  $\alpha$  and  $\nu$  are the critical exponents,  $f(z)$  is a scaling function, and constant  $C_0$  represents the analytical background contribution at  $t \rightarrow 0$ . We consider scaling regimes, where  $z = tL^{1/\nu}$  is some constant at  $t \rightarrow 0$ . It is true for the  $C_V$  scaling at  $\beta = \tilde{\beta}_c(L)$ , as well as at  $\beta = \hat{\beta}_c(L)$ . Thus, we have  $t = zL^{-1/\nu}$  at  $t \rightarrow 0$  or  $L \rightarrow \infty$ . Inserting this relation into (3.1), we obtain the following asymptotic ansatz

$$C_V = C_0 + AL^{\alpha/\nu} \quad \text{at } L \rightarrow \infty, \quad (3.2)$$

where  $A = |z|^{-\alpha} f(z)$  is a constant, which depends only on the asymptotic value of  $z$ , whereas  $C_0$  is the same constant as in (3.1), which is independent of  $z$ .

For finite values of  $t$ , corrections to scaling are considered. These are corrections  $|t|^{-\alpha+\theta} f_1(tL^{1/\nu})$ ,  $|t|^{-\alpha+2\theta} f_2(tL^{1/\nu})$ , etc., where  $\theta$  is the correction-to-scaling exponent, as well as analytic corrections  $C_1 t + C_2 t^2 + \dots$ . Since  $2\theta - \alpha < 1$  holds according to the estimates of the perturbative RG theory ( $\theta \simeq 0.5$ ,  $\alpha \simeq 0.11$ ), the two most important correction terms in (3.1) are  $\sim |t|^{-\alpha+\theta}$  and  $\sim |t|^{-\alpha+2\theta}$ . The corresponding corrections in (3.2) are  $\propto L^{(\alpha/\nu)-\omega}$  and  $\propto L^{(\alpha/\nu)-2\omega}$ , where  $\omega = \theta/\nu$ . One has to note that there can exist also correction terms, which are described by correction-to-scaling exponents of higher orders, i.e.,  $\theta_1 > \theta$ ,  $\theta_2 > \theta_1$ , etc. In particular, the exponents  $\theta = 0.54 \pm 0.05$ ,  $\theta_1 = 1.5 \pm 0.3$  and  $\theta_2 = 1.67 \pm 0.11$  (denoted as  $\Delta_{400}$ ,  $\Delta_{500}$  and  $\Delta_{422}$ ) have been found for the 3D Ising model in [21]. However, since  $\theta_1 > 2\theta$  holds, the additional correction terms  $\sim |t|^{-\alpha+\theta_1}$  and  $\sim |t|^{-\alpha+\theta_2}$ , as well as higher-order terms with  $\theta_1$  and  $\theta_2$ , are negligible as compared to  $\sim |t|^{-\alpha+\theta}$  and  $\sim |t|^{-\alpha+2\theta}$  at  $t \rightarrow 0$ .

We have fitted our  $C_V$  data at  $\beta = \tilde{\beta}_c(L)$  ( $U = 1.6$ ) and at  $\beta = \hat{\beta}_c(L)$  (the  $C_V^{\max}$  data) to the ansatz (3.2) with fixed  $\alpha/\nu = 0.173$ , in accordance with the known perturbative RG estimates  $\alpha = 0.109 \pm 0.004$  and  $\nu = 0.6304 \pm 0.0013$  [13], i.e.,  $\alpha/\nu = 0.173 \pm 0.007$ . According to the derivation of (3.2) from (3.1),  $C_0$  has the same value in these two cases, if the power-law scaling (3.2) with the RG exponent  $\alpha/\nu \simeq 0.173$  is correct at  $L \rightarrow \infty$ . Our aim is to test it by fitting the two data sets and looking whether the estimates of  $C_0$  become consistent at large enough sizes.

We have evaluated  $C_0$  from fits within  $[L/a, aL]$  and have plotted the results as functions of  $L^{(\alpha/\nu)-\omega}$  with  $\omega = 0.8$ , using the perturbative RG estimate  $\omega = 0.799 \pm 0.011$  [13]. Here  $aL \in \mathbb{N}$ , and  $a = \sqrt{2}, 2, \sqrt{8}, 4$ , etc., can be chosen. A smaller  $a$  value allows to make estimations closer to the thermodynamic limit, but the statistical errors decrease for larger  $a$  values. We have set  $a = \sqrt{8}$  as an optimal choice for our data. In fact,  $C_0 = C_0(L)$  is an effective coefficient, and its convergence to the asymptotic value is expected to be linear in  $L^{(\alpha/\nu)-\omega}$  at  $L \rightarrow \infty$ . Indeed, if the data are consistent with  $C_V(\tilde{L}) = C_0 + A\tilde{L}^{\alpha/\nu} + \mathcal{O}(\tilde{L}^{(\alpha/\nu)-\omega})$ , and we fit these data to the ansatz  $C_V(\tilde{L}) = C_0 + A\tilde{L}^{\alpha/\nu}$  within  $\tilde{L} \in [L/a, aL]$ , then the correction term  $\mathcal{O}(\tilde{L}^{(\alpha/\nu)-\omega})$  is approximately compensated by certain shifts in  $C_0$  and  $A$  values such that  $C_0(L) = C_0 + \delta C_0(L)$  and  $A(L) = A + \delta A(L)$ . Obviously, the best approximation (minimizing the  $\chi^2$  of the fit) is such that the compensating terms  $\delta C_0(L)$  and  $\delta A(L)\tilde{L}^{\alpha/\nu}$  are comparable with  $\mathcal{O}(\tilde{L}^{(\alpha/\nu)-\omega})$  within  $\tilde{L} \in [L/a, aL]$ . It means that  $C_0(L) = C_0 + \mathcal{O}(L^{(\alpha/\nu)-\omega})$  holds.

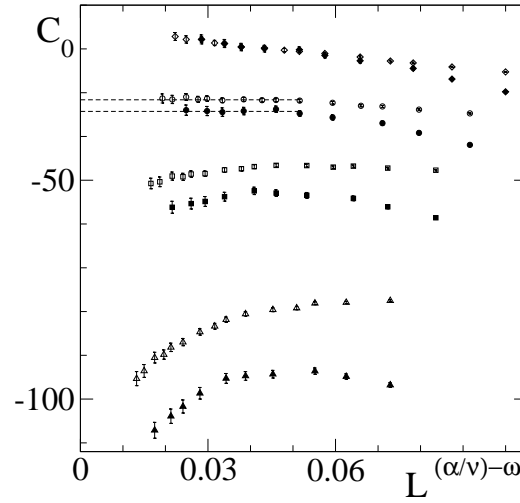


Figure 3: The constant background term  $C_0$  in (3.2) depending on  $L^{(\alpha/\nu)-\omega}$  at  $\omega=0.8$ , evaluated from fits within  $[L/\sqrt{8}, \sqrt{8}L]$  with fixed exponent ratio  $\alpha/\nu=0.113$  (triangles),  $\alpha/\nu=0.149$  (squares),  $\alpha/\nu=0.173$  (circles) and  $\alpha/\nu=0.196$  (diamonds). Empty symbols refer to the  $C_V$  data at  $\beta=\tilde{\beta}_c(L)$ , corresponding to  $U=1.6$ , whereas solid symbols — to the  $C_V^{\max}$  data. Dashed lines indicate the systematic shift between the two plots at  $\alpha/\nu=0.173$ .

The  $C_0(L)$  plots for  $C_V$  data at  $\beta=\tilde{\beta}_c(L)$  and for  $C_V^{\max}$  data at  $\alpha/\nu=0.173$  are shown in Fig. 3 by empty circles and solid circles, respectively. The plots tend to saturate at certain values, shown by dashed lines. However, these values differ from each other:  $-31.63(30)$  in the first case and  $-34.27(58)$  in the second case. The discrepancy is  $\Delta C_0=2.64(65)$ . This inconsistency is removed, assuming that the correct  $\alpha/\nu$  value is different from 0.173. Indeed, we observe that the two plots tend to merge very accurately and lie practically on top of each other for  $\sqrt{8}L \geq 320$  at  $\alpha/\nu=0.196(6)$  — see the upper plots (diamonds) in Fig. 3. The precise merging point has been determined as the value of  $\alpha/\nu$  at which linear fits are consistent within  $320 \leq \sqrt{8}L \leq 1024$ . For a more complete picture, we have shown in Fig. 3 also the plots for  $\alpha/\nu=0.149$  and  $\alpha/\nu=0.113$ . These values come from a direct estimation of  $\alpha/\nu$  in Section 4, where  $\alpha/\nu=0.149(38)$  appears as a maximal value and  $\alpha/\nu=0.113(30)$  — as a minimal value obtained there. As we can see, the systematic shift between two plots at  $\alpha/\nu=0.149$  and, particularly, at  $\alpha/\nu=0.113$  is remarkably larger than the shift at  $\alpha/\nu=0.173$ .

The effect of corrections to scaling can be evaluated from the magnitude of variations in  $C_0(L)$ . Apparently, corrections to scaling are very small or negligible for the discrepancy  $\Delta C_0(L)$  between the two plots at a given  $\alpha/\nu$ . Indeed,  $\Delta C_0(L)$  is almost constant within a sufficiently wide range of small  $L^{(\alpha/\nu)-0.8}$  values. Therefore, our method is well justified for finding the  $\alpha/\nu$  value at which  $\lim_{L \rightarrow \infty} \Delta C_0(L) = 0$  holds if  $\omega$  is, indeed, as large as  $\omega \approx 0.8$ . The obtained result  $\alpha/\nu=0.196(6)$  remarkably deviates from the perturbative RG value  $0.173 \pm 0.007$ . It suggests that the perturbative RG value is underestimated, whereas the direct estimation in Section 4 suggests that it, more likely, is

either overestimated or correct within the error bars. Consequently, if we are looking for an average estimate of  $\alpha/\nu$  (assuming that the power-law ansatz holds), then it could be still consistent with the RG value  $0.173 \pm 0.007$ . However, a question arises about the inconsistency between different estimations.

Our scaling consistency test in Fig. 3 refers only to  $U = \langle m^4 \rangle / \langle m^2 \rangle^2 = 1.6$ . It would be interesting to see how the value of  $\alpha/\nu$ , at which the  $C_0(L)$  curves collapse, is changed when the pseudocritical coupling is determined at a different value of  $U$ . Following the method of [15], our simulations have been performed for a set of  $\beta$  values in vicinity of  $\tilde{\beta}_c(L)$ , corresponding to  $U = 1.6$ . This method allows us to recalculate the results for any coupling, which is close enough to  $\tilde{\beta}_c(L)$ . In particular, using the Taylor series expansion of  $\ln \langle m^2 \rangle$  and  $\ln \langle m^4 \rangle$  up to the third order, we have evaluated  $\beta = \tilde{\beta}_c(L)$  for which  $U = 1.7$  holds. Furthermore, using the Taylor series expansion of  $\ln \langle -\varepsilon \rangle$  and  $\ln \langle \varepsilon^2 \rangle$  up to the second order, we have recalculated the specific heat values at  $\beta = \tilde{\beta}_c(L)$  within  $32 \leq L \leq 864$ . We have considered a series of approximations, where the  $n$ -th approximation includes terms up to the  $n$ -th order in the expansion of  $\ln \langle -\varepsilon \rangle$  and  $\ln \langle \varepsilon^2 \rangle$  and terms up to the  $(n+1)$ -th order in the expansion of  $\ln \langle m^2 \rangle$  and  $\ln \langle m^4 \rangle$ . The chosen here orders are not equal, since the evaluated derivatives are statistically more reliable in the second case. The validity of this recalculation is confirmed by a fast enough convergence of the Taylor series, as well as by an observation that the recalculated data are well consistent with the results of direct simulations for  $\beta = \tilde{\beta}_c(L)$  within  $32 \leq L \leq 64$ . For example, at  $L = 64$ , the series of approximations for  $C_V$  is 55.162(83), 50.490(87) and 50.406(88), corresponding to  $n = 0$ ,  $n = 1$  and  $n = 2$ . The direct simulation yields  $C_V = 50.298(83)$  in this case. The recalculated value of  $\tilde{\beta}_c(64)$  is 0.22158995(59), whereas that of the direct simulation is 0.22159001(51). No extra simulations have been performed for  $64 < L \leq 864$ . However, the observed convergence of the Taylor series is fast in this case, the difference between approximations with  $n = 1$  and  $n = 2$  being smaller than one standard deviation. We have restricted our calculation to  $32 \leq L \leq 864$ , since a remarkable increase of this difference has been observed outside of this interval.

Note that  $U$  is about 1.2 for the  $C_V^{\max}$  data (i.e., at  $\beta = \hat{\beta}_c(L)$ ), and it corresponds to  $\beta > \beta_c \simeq 0.2216546$ , whereas  $U = 1.6$  corresponds to  $\beta$  near  $\beta_c$  (because  $U^* \approx 1.6$  is the critical value of  $U$ ). Hence, our recalculated data for  $U = 1.7$  refer to the region  $\beta < \beta_c$ . The results of our scaling test for  $U = 1.7$  are shown in Fig. 4. The discrepancy at  $\alpha/\nu = 0.173$  is  $\Delta C_0 = 2.95(67)$ , which slightly exceeds the value 2.64(65) found for  $U = 1.6$ . The collapse of these  $C_0(L)$  plots takes place at  $\alpha/\nu = 0.193(5)$ , as shown by diamonds in Fig. 4. This value is slightly smaller than 0.196(6) found for  $U = 1.6$ . Since the data of  $U = 1.7$  have been recalculated from those of  $U = 1.6$ , the small changes in our estimates are mainly of systematical character, showing how the results are varied with  $U$ . The reason why the estimated merging point ( $\alpha/\nu$  value) has a smaller error at  $U = 1.7$  than at  $U = 1.6$  is the fact that the discrepancy  $\Delta C_0$  is varied more rapidly with  $\alpha/\nu$  at  $U = 1.7$ .

We have performed the consistency test also for relatively small lattices sizes by fitting the  $C_V$  data at  $\beta = \tilde{\beta}_c(L)$  ( $U = 1.6$ ) and the  $C_V^{\max}$  data to the ansatz to (3.2) within  $L \in [L_{\min}, L_{\max}]$  with relatively small lattice sizes  $L_{\min} = 32$  and  $L_{\max} = 64$ . We have determined



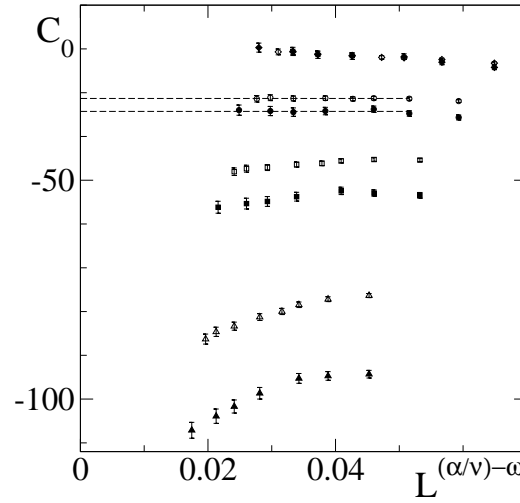


Figure 4: The constant background term  $C_0$  in (3.2) depending on  $L^{(\alpha/\nu)-\omega}$  at  $\omega=0.8$ , evaluated from fits within  $[L/\sqrt{8}, \sqrt{8}L]$  with fixed exponent ratio  $\alpha/\nu=0.113$  (triangles),  $\alpha/\nu=0.149$  (squares),  $\alpha/\nu=0.173$  (circles) and  $\alpha/\nu=0.193$  (diamonds). Empty symbols refer to the  $C_V$  data at  $\beta=\tilde{\beta}_c(L)$ , corresponding to  $U=1.7$ , whereas solid symbols — to the  $C_V^{\max}$  data. Dashed lines indicate the systematic shift between the two plots at  $\alpha/\nu=0.173$ .

the  $\alpha/\nu$  value, at which both data sets give consistent background term  $C_0$ , and have determined this value of  $C_0$ . Then we have examined how the results are varied if the maximal lattice size  $L_{\max}$  increases. The results of this test are collected in Table 3. For relatively small  $L_{\min}$  and  $L_{\max}$ , these estimates of  $\alpha/\nu$  are systematically larger than the value 0.196(6) obtained before. However, these estimates are well consistent with  $\alpha/\nu=0.196(6)$  for large  $L_{\max}$ . Note, however, that the quality of the actual fits with fixed  $L_{\min}=32$  are quite low. For example, we have  $\chi^2/\text{d.o.f.}=3.31$  for the data at  $\beta=\tilde{\beta}_c(L)$  and  $\chi^2/\text{d.o.f.}=4.15$  for the  $C_V^{\max}$  data at  $L_{\max}=1024$ . The fit quality at  $L_{\max}=1024$  is improved for larger  $L_{\min}$  values. For example, at  $L_{\min}=48$  we obtain  $\alpha/\nu=0.1887(51)$  and  $C_0=$

Table 3: The values of  $\alpha/\nu$  at which the two data sets (the  $C_V$  data at  $\beta=\tilde{\beta}_c(L)$  and the  $C_V^{\max}$  data) give the same value of  $C_0$  if fitted to the ansatz (3.2) within  $L \in [L_{\min}, L_{\max}]$ . The results for  $\alpha/\nu$  and  $C_0$  are shown depending on  $L_{\max}$  at a fixed  $L_{\min}=32$ .

$L_{\max}$	$\alpha/\nu$	$C_0$	$L_{\max}$	$\alpha/\nu$	$C_0$
64	0.258(21)	-6.5(4.8)	320	0.2038(57)	-18.7(2.2)
80	0.230(15)	-12.2(4.4)	384	0.2022(52)	-19.2(2.1)
96	0.220(12)	-14.9(3.8)	512	0.2043(50)	-18.0(2.0)
128	0.2077(93)	-18.3(3.4)	640	0.2005(47)	-19.3(2.0)
160	0.2039(77)	-19.4(2.9)	768	0.1991(43)	-19.8(1.8)
192	0.2006(66)	-20.3(2.6)	1024	0.1966(39)	-20.7(1.7)
256	0.2053(61)	-18.3(2.3)			

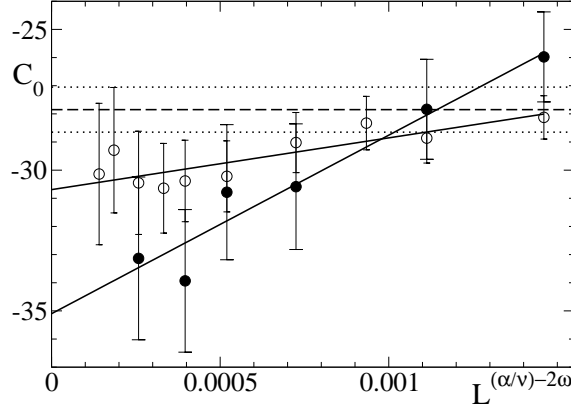


Figure 5: The constant background term  $C_0$  in (3.3) depending on  $L^{(\alpha/\nu)-2\omega}$  at  $\omega = 0.832$ , evaluated from fits within  $[L/4, 4L]$  with fixed  $\alpha/\nu = 0.174$  and  $\omega = 0.832$ . Empty circles correspond to the  $C_V$  data at  $\beta = \tilde{\beta}_c(L)$ , whereas solid circles — to the  $C_V^{\max}$  data. Linear fits are shown by solid straight lines. The horizontal dashed line indicates the value  $-27.85 \pm 0.80$  of [5], and the dotted lines indicate the range of error bars  $\pm 0.80$ .

$-23.3(2.6)$  with  $\chi^2/\text{d.o.f.} = 0.80$  and  $\chi^2/\text{d.o.f.} = 1.44$  for these two data sets. At  $L_{\min} = 96$ , the corresponding estimates are  $\alpha/\nu = 0.1915(84)$  and  $C_0 = -20.8(4.6)$  with  $\chi^2/\text{d.o.f.} = 0.54$  and  $\chi^2/\text{d.o.f.} = 1.63$ .

As an extra test, we have performed an estimation of the constant  $C_0$ , using the ansatz

$$C_V = C_0 + AL^{\alpha/\nu} (1 + bL^{-\omega}) \quad (3.3)$$

instead of (3.2). In order to compare the results with the estimate  $C_0 = -27.85 \pm 0.80$  of [5], we have performed fits with  $\alpha/\nu = 0.174$  and  $\omega = 0.832$ , in agreement with the values of the critical exponents considered in [5]. It is not clear a priori whether the refined ansatz (3.3) will give better results than (3.2), because statistical errors become rather large when the correction term  $bL^{-0.832}$  is included, and one needs to include smaller sizes  $L$  to reach an acceptable statistical accuracy. Moreover, the fit results depend remarkably on the chosen interval of sizes. For example, by fitting the data of Table 2 within  $L \in [L_{\min}, 1024]$ , we obtain  $C_0 = -26.35(86)$  at  $L_{\min} = 16$ ,  $C_0 = -29.3(1.6)$  at  $L_{\min} = 32$  and  $C_0 = -33.1(2.9)$  at  $L_{\min} = 64$ . Such effects can be studied in a systematic way by fitting the data within  $[L/a, aL]$  and considering how the results are varied. Indeed, the obtained in this way estimate  $C_0(L)$  has certain expected scaling. By similar arguments as in the case of the ansatz (3.2), we find that this scaling is linear in  $L^{(\alpha/\nu)-2\omega}$  at  $L \rightarrow \infty$  because of the influence of the remainder term  $\mathcal{O}(L^{(\alpha/\nu)-2\omega})$ . We have evaluated  $C_0(L)$  by fitting the data within  $[L/4, 4L]$ . The  $C_0(L)$  vs  $L^{(\alpha/\nu)-2\omega}$  plots for both data sets (in Tables 1 and 2) show certain systematic variations — see Fig. 5. These plots are perfectly fit by straight lines, yielding the asymptotic estimates  $C_0 = -30.7(1.6)$  from the data at  $\beta = \tilde{\beta}_c(L)$  (Table 1) and  $C_0 = -35.1(3.0)$  — from the  $C_V^{\max}$  data (Table 2). Thus, the discrepancy is  $\Delta C_0 = 4.4(3.4)$ . Because of the large statistical errors, it is impossible to draw a strict

conclusion that  $\Delta C_0 \neq 0$ . However, it is clear that the estimate  $C_0 = -35.1(3.0)$ , extracted from the  $C_V^{\max}$  data, is not well consistent with the value  $-27.85 \pm 0.80$  of [5].

At  $\alpha/\nu = 0.173$  and  $\omega = 0.8$ , this method yields  $C_0 = -31.6(1.7)$ , using the data at  $\beta = \tilde{\beta}_c(L)$ , and  $C_0 = -36.4(3.2)$ , using the  $C_V^{\max}$  data. These estimates agree with the corresponding values,  $C_0 = -31.63(30)$  and  $C_0 = -34.27(58)$ , obtained from the ansatz (3.2).

#### 4 Direct estimation of $\alpha/\nu$

We have evaluated the exponent ratio  $\alpha/\nu$  also as a fit parameter in (3.2). The fits within  $[L/\sqrt{8}, \sqrt{8}L]$  give effective exponents  $(\alpha/\nu)_{\text{eff}}$  plotted in Fig. 6. Because of the influence of the neglected in (3.2) correction term, which is by a factor  $\mathcal{O}(L^{-\omega})$  smaller than the leading term, the effective exponent depends on  $L$  and is expected to be linear in  $L^{-\omega}$  at  $L \rightarrow \infty$ . The shown here linear and quadratic fits of  $(\alpha/\nu)_{\text{eff}}$  vs  $L^{-0.8}$  correspond to the  $C_V$  data at  $\beta = \tilde{\beta}_c(L)$ . They give  $\alpha/\nu = 0.149(38)$  and  $\alpha/\nu = 0.139(50)$ , respectively. Such fits are not good and plausible enough for the effective exponents, extracted from the  $C_V^{\max}$  data (asterisks in Fig. 6). However, these effective exponents decrease for large  $L$ , suggesting that  $\alpha/\nu$  is smaller than the value  $0.196(6)$  obtained from the consistency test in Section 3. The largest- $L$  estimate is  $0.113(30)$ , as provided by the fit over  $L \in [128, 1024]$  with  $\chi^2/\text{d.o.f.} = 1.08$ . Because of the decreasing,  $\alpha/\nu$  could be even smaller than  $0.113(30)$ .

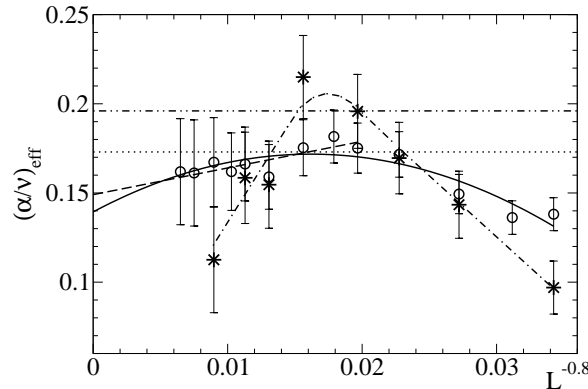


Figure 6: The effective exponent  $(\alpha/\nu)_{\text{eff}}$  depending on  $L^{-0.8}$ , evaluated from fits to (3.2) within  $[L/\sqrt{8}, \sqrt{8}L]$ . Circles correspond to the  $C_V$  data at  $\beta = \tilde{\beta}_c(L)$ , asterisks — to the  $C_V^{\max}$  data. Linear and quadratic fits of circles are shown by dashed line and solid line, respectively. The dot-dashed line is a guide to eye for asterisks. The horizontal lines indicate the RG value  $0.173$  (dotted line) and the value  $0.196$  (dot-dot-dashed line), obtained from the scaling test in Section 3.

We have considered also the  $C_V$  fits within  $L \geq L_{\min}$ , including corrections to scaling with  $\omega = 0.8$ . At large enough  $L_{\min}$ , the fit results agree well with those provided by the effective exponents. For example, the fits of the  $C_V$  data at  $\beta = \tilde{\beta}_c(L)$  to

$$C_V = C_0 + AL^{\alpha/\nu} (1 + a_1 L^{-\omega} + a_2 L^{-2\omega}) \quad (4.1)$$

give  $\alpha/\nu=0.147(40)$  at  $L_{\min}=27$  and  $\alpha/\nu=0.136(49)$  at  $L_{\min}=32$ . Such fits of  $C_V^{\max}$  data give  $\alpha/\nu=0.139(53)$  at  $L_{\min}=20$  and  $\alpha/\nu=0.124(67)$  at  $L_{\min}=24$ .

## 5 Test of the logarithmic scaling

We have tested also the GFD theory [10]. According to [10, 22],  $C_V$  has a logarithmic singularity

$$C_V = C_0 + \ln(|t|/t_0) f(tL^{1/\nu}) \quad \text{at } t \rightarrow 0 \quad (5.1)$$

for any given  $tL^{1/\nu}$ , where the scale parameter  $t_0$  is included to ensure that  $C_V$  can be represented in this form at an arbitrary rescaling  $t \rightarrow st$ . It corresponds to

$$C_V = A \ln L + B \quad \text{at } L \rightarrow \infty \quad (5.2)$$

at a fixed  $z = tL^{1/\nu} \neq 0$ , which holds asymptotically for  $\beta = \tilde{\beta}_c(L)$  and  $\beta = \hat{\beta}_c(L)$ . Here  $B = B(z) \neq C_0$ . The expected form, including corrections to scaling, is

$$C_V = A \ln L (1 + \mathcal{O}(L^{-\omega})) + B (1 + \mathcal{O}(L^{-\omega})). \quad (5.3)$$

It is consistent with the  $C_V^{\max}$  behavior in the 2D case [23], where  $\omega=1$ . In our case  $\omega=1/8$  is expected [8, 10, 29].

To test the logarithmic scaling scenario, we have evaluated the  $\chi^2/\text{d.o.f.}$  of the three-parameter fits

$$C_V = A \ln L (1 + aL^{-1/8}) + B \quad (5.4)$$

within  $L \geq L_{\min}$  and have compared them with the  $\chi^2/\text{d.o.f.}$  values for the power-law ansatz

$$C_V = C_0 + AL^{\alpha/\nu} (1 + aL^{-0.8}) \quad (5.5)$$

with fixed  $\alpha/\nu = 0.173$  or  $\alpha/\nu = 0.196$  — see Table 4. The logarithmic ansatz is good enough for  $L_{\min} \geq 48$ , since  $\chi^2/\text{d.o.f.}$  is about unity for moderately good fits [24]. Thus, (5.4) can be the correct asymptotic ansatz. The power-law ansatz (5.5) provides better fits for the  $C_V$  data at  $\beta = \tilde{\beta}_c(L)$  and worse (relatively poor) fits for the  $C_V^{\max}$  data at  $L_{\min} \geq 48$ .

Table 4: The values of  $\chi^2/\text{d.o.f.}$  depending on  $L_{\min}$  for three different fits within  $L \geq L_{\min}$ . Fits 1 and 2 are the fits to ansatz (5.5) with fixed exponents  $\alpha/\nu=0.173$  (fit 1) or  $\alpha/\nu=0.196$  (fit 2). Fit 3 is the fit to ansatz (5.4). The results of two data sets are presented: set 1 — the  $C_V$  data at  $\beta = \tilde{\beta}_c(L)$  and set 2 — the  $C_V^{\max}$  data.

$L_{\min}$	$\chi^2/\text{d.o.f.}$ of set 1			$\chi^2/\text{d.o.f.}$ of set 2		
	fit 1	fit 2	fit 3	fit 1	fit 2	fit 3
32	0.48	0.43	2.43	1.47	1.43	2.46
48	0.39	0.44	0.92	1.28	1.41	1.14
64	0.43	0.49	0.63	1.40	1.55	1.03
96	0.38	0.39	0.49	1.40	1.47	1.17

## 6 Summary and conclusions

We have systematically analyzed the MC data for specific heat of the 3D Ising model on large lattices:  $L \leq 1536$  at  $\beta = \tilde{\beta}_c(L)$  and  $L \leq 1024$  at  $\beta = \hat{\beta}_c(L)$ . Fits of these two data sets (as illustrated in Fig. 3) provide consistent values of  $C_0$  in (3.2) at  $\alpha/\nu = 0.196(6)$ , whereas the perturbative RG estimate is  $0.173 \pm 0.007$ . An extra scaling test, where the pseudocritical coupling  $\tilde{\beta}_c(L)$  is replaced by  $\bar{\beta}_c(L)$ , evaluated at  $U = \langle m^4 \rangle / \langle m^2 \rangle^2 = 1.7$  instead of  $U = 1.6$ , gives  $\alpha/\nu = 0.193(5)$ . Several estimations of this kind have been discussed in Section 3, giving results consistent with  $\alpha/\nu = 0.196(6)$  within the error bars. However, a direct estimation of  $\alpha/\nu$  from  $C_V^{\max}$  data suggests that  $\alpha/\nu$  is  $0.113(30)$  or even smaller. These MC estimations are well justified if the correction-to-scaling exponent  $\omega$  is as large as usually assumed, i.e.,  $\omega \approx 0.8$ . Because of the inconsistencies in  $\alpha/\nu$  values, it is difficult to give a good interpretation of the data by a power-law ansatz if  $\omega \approx 0.8$ . Thus, the power-law scaling of the perturbative RG theory can be challenged in view of this fact. It can be also questioned whether the large in magnitude negative values ( $-31.63(30)$  and  $-34.27(58)$ ) of the analytic background contribution  $C_0$ , obtained at  $\alpha/\nu = 0.173$ , are physically reasonable.

We have found that the data are well consistent with the logarithmic ansatz (5.4) of the GFD theory (see [10,22]) for large enough system sizes  $L \geq 48$ .

There are many numerical evidences (see, e.g. [20]) supporting the critical exponents of the perturbative RG theory. These include the results of the high temperature series expansion (see, e.g., [25–27]), as well as the MC analysis (see, e.g., [1–7,28]). As argued in [8], we should mainly rely on non-perturbative methods, i.e., the MC method in the case of the 3D Ising model. Monte Carlo evidences for the singularity of specific are mainly based on an estimation of the exponent  $\nu$ , calculating  $\alpha$  from the hyperscaling relation  $\alpha + d\nu = 2$ . We have estimated  $\alpha/\nu$  directly from specific heat data. Moreover, according to our knowledge, the scaling test in Section 3 has never been performed before. The linear lattice sizes in our simulations exceed by an order of magnitude those simulated and analyzed earlier by other authors. Thus, our current results provide a rather serious numerical evidence, according to which the logarithmic scaling (5.4) of specific heat provides a remarkably better interpretation of the data than the usual RG scaling. Our results do not imply that something is wrong with the previous MC simulations, but only indicate that the usually considered sizes  $L \leq 128$  are too small for a reliable estimation of the critical exponents.

Corrections to scaling with small exponents  $\omega = 1/8$  or  $\theta = 1/12$ , predicted for the 3D Ising model by the GFD theory, well explain the fact that numerically estimated critical exponents can remarkably depend on the considered range of sizes  $L$  or range of reduced temperatures  $t$  even for very large  $L$  or very small  $t$ . Such possible corrections to scaling have never been considered in earlier numerical studies by other authors. Inclusion of such corrections can potentially resolve all the apparent inconsistencies between various numerical estimations of the critical exponents, including our MC analysis and other possible MC analyses of large enough lattices.

At small  $\omega$  (such as  $\omega = 1/8$ ), a very slow crossover from certain effective scaling behavior to the true critical scaling behavior is possible. Here by “effective scaling behavior” we mean such a behavior, which is well described by certain effective exponents, which are different from the true critical exponents. If the crossover effect is ignored, then the numerically estimated critical exponents can be consistent with these effective exponents. In principle, it can explain the discrepancies between the known numerical estimates  $\nu \approx 0.63$  and  $\eta \approx 0.037$  (e.g.,  $\nu = 0.63020(12)$  and  $\eta = 0.0368(2)$  [5]), obtained for the 3D Ising universality class by ignoring such a possible crossover effect, and the values  $\nu = 2/3$ ,  $\eta = \omega = 1/8$  of the GFD theory. However, it would imply that the numerically obtained effective exponents are almost universal, since the known numerical estimates of the critical exponents for various models of the 3D universality class are consistent. It can rise serious questions about the validity of this tentative explanation. On the other hand, one can argue that the numerical estimation of the critical exponents is not a very strict and rigorous method. In particular, some problems have been revealed and discussed in [30, 31], where it has been stated that an analysis of the critical behavior points to distinct high- and low-temperature exponents, especially for the specific heat, although the agreement is good between different lattices.

Our tentative explanation seems to be very reasonable from the point of view of certain rigorously proven statement in [29], showing that the leading correction to scaling in the two-point correlation function of the  $\varphi^4$  model is given by the exponent  $\theta = \omega\nu \leq \gamma - 1$ , if  $\gamma > 1$  and certain general (conventional) scaling arguments hold (see Section 3 in this paper). According to the known numerical estimates,  $\theta$  for the 3D Ising universality class (including also the scalar  $\varphi^4$  model) is about 0.52 (see, e.g., [5]), whereas  $\gamma - 1 \approx 0.24$ . It seems that this contradiction can be reasonably explained only if we assume that the above outlined crossover scenario really holds. This controversy requires a further investigation and discussion.

## Acknowledgments

This work was made possible by the facilities of the Shared Hierarchical Academic Research Computing Network (SHARCNET: [www.sharcnet.ca](http://www.sharcnet.ca)). It has been performed within the framework of the ESF Project No. 1DP/1.1.1.2.0/09/ APIA/VIAA/142, and with the financial support of this project. R. M. acknowledges the support from the NSERC and CRC program.

## References

- [1] M. Hasenbusch, Int. J. Mod. Phys. C 12 (2001) 911.
- [2] Y. Deng, H. W. J. Blöte, Phys. Rev. E 68 (2003) 036125.
- [3] J.-H. Chen, M. E. Fisher, Phys. Rev. Lett. 48 (1982) 630.
- [4] H. W. J. Blöte, E. Luijten, J. R. Heringa, J. Phys. A: Math. Gen. 28 (1995) 6289.
- [5] X. Feng, H. W. J. Blöte, Phys. Rev. E 81 (2010) 031103.

- [6] M. Hasenbusch, Phys. Rev. B 82 (2010) 174433.
- [7] M. Hasenbusch, Phys. Rev. B 82 (2010) 174434.
- [8] J. Kaupužs, J. Rimšāns, R. V. N. Melnik, Ukr. J. Phys. 56 (2011) 845.
- [9] D. Stauffer, Braz. J. Phys. 30 (2000) 787.
- [10] J. Kaupužs, Ann. Phys. (Berlin) 10 (2001) 299.
- [11] J. Kaupužs, Progress of Theoretical Physics 124 (2010) 613.
- [12] Z.-D. Zhang, Philosophical Magazine 87 (2007) 5309.
- [13] R. Guida, J. Zinn-Justin, J. Phys. A 31 (1998) 8103.
- [14] U. Wolff, Phys. Rev. Lett. 62 (1989) 361.
- [15] J. Kaupužs, J. Rimšāns, R. V. N. Melnik, Phys. Rev. E 81 (2010) 026701.
- [16] D. J. Amit, Field Theory, the Renormalization Group, and Critical Phenomena, World Scientific, Singapore, 1984.
- [17] S.-K. Ma, Modern Theory of Critical Phenomena, W. A. Benjamin, Inc., New York, 1976.
- [18] J. Zinn-Justin, Quantum Field Theory and Critical Phenomena, Clarendon Press, Oxford, 1996.
- [19] H. Kleinert, V. Schulte-Frohlinde, Critical Properties of  $\phi^4$  Theories, World Scientific, Singapore, 2001.
- [20] A. Pelissetto, E. Vicari, Phys. Rep. 368 (2002) 549.
- [21] K. E. Newman, E. K. Riedel, Phys. Rev. B 30 (1984) 6615.
- [22] A. L. Tseskis, J. Exp. Theor. Phys. 75 (1992) 269.
- [23] W. Janke, R. Kenna, Nucl. Phys. Proc. Suppl. 106 (2002) 929.
- [24] W. H. Press, B. P. Flannery, S. A. Teukolsky, W. T. Vetterling, Numerical Recipes – The Art of Scientific Computing, Cambridge University Press, Cambridge, 1989.
- [25] M. Campostrini, A. Pelissetto, P. Rossi, E. Vicari, Phys. Rev. E 65 (2002) 066127.
- [26] P. Butera, M. Comi, Phys. Rev. B 65 (2002) 144431.
- [27] P. Butera, M. Comi, Phys. Rev. B 72 (2005) 014442.
- [28] M. Collura, J. Stat. Mech. (2010) P12036.
- [29] J. Kaupužs, Can. J. Phys. 90 (2012) 373.
- [30] R. Häggkvist, A. Rosengren, P. H. Lundow, K. Markström, D. Andrén, P. Kundrotas, Advances in Physics 56 (2007) 653.
- [31] P. H. Lundow, K. Markström, A. Rosengren, Philosophical Magazine 89 (2009) 2009.